Mon. Not. R. Astron. Soc. **351,** 630–642 (2004) doi:10.1111/j.1365-2966.2004.07811.x

# Testing the locality of transport in self-gravitating accretion discs

G. Lodato[1]★ and W. K. M. Rice[2]

[1]*Institute of Astronomy, Madingley Road, Cambridge CB3 0HA*
[2]*School of Physics and Astronomy, University of St Andrews, North Haugh, St Andrews, Fife KY16 9SS*

Accepted 2004 March 4. Received 2004 March 1; in original form 2003 October 23

**ABSTRACT**

In this paper, we examine the issue of characterizing the transport associated with gravitational instabilities in relatively cold discs, discussing in particular the conditions under which it can be described within a local, viscous framework. We present the results of global, three-dimensional, smoothed particle hydrodynamics simulations of self-gravitating accretion discs, in which the disc is cooled using a simple parametrization for the cooling function. Our simulations show that the disc settles in a 'self-regulated' state, where the axisymmetric stability parameter $Q \approx 1$ and where transport and energy dissipation are dominated by self-gravity. We have computed the gravitational stress tensor and compared our results with expectations based on a local theory of transport. We find that, as long as the disc mass is smaller than $0.25 M_\star$ and the aspect ratio $H/R \lesssim 0.1$, transport is determined locally, thus allowing for a viscous treatment of the disc evolution.

**Key words:** accretion, accretion discs – gravitation – instabilities – stars: formation – galaxies: active.

## 1 INTRODUCTION

One of the basic unknowns of accretion disc theory is the physical mechanism ultimately responsible for angular momentum transport and energy dissipation in the disc. It is well known that classical hydrodynamical viscosity is not sufficient to provide accretion at the rates inferred from the observations in almost every astrophysical context where accretion discs play a role. The usual way to overcome this difficulty is to assume that transport is dominated by some 'anomalous' viscous phenomenon, possibly related to collective instabilities in the disc, and to give some ad hoc parametrizations for the viscosity. The most widely used of such parametrizations is the so-called $\alpha$-prescription (Shakura & Sunyaev 1973, see Section 2).

It has been recently recognized that accretion discs threaded by a weak magnetic field are subject to magnetohydrodynamics (MHD) instabilities (see Balbus & Hawley 1998, and references therein), which can induce turbulence in the disc, thereby being able to transport angular momentum and to promote the accretion process. However, in many astrophysically interesting cases, such as the outer regions of protostellar discs, the ionization level is expected to be low, reducing significantly the effects of magnetic fields in determining the dynamics of the disc, at least over limited radial ranges (Gammie 1996). A possible alternative source of transport in cold discs is provided by gravitational instabilities (Lin & Pringle 1987; Laughlin & Bodenheimer 1994; Armitage, Livio & Pringle 2001). Moreover, in environments where the disc mass is a significant fraction of the central object mass, such as during the assembly of protostellar discs, it is inevitable that disc self-gravity will play a role.

The axisymmetric stability of a thin disc with respect to its own self-gravity is determined by the parameter $Q$ (Toomre 1964), defined as

$$Q = \frac{c_s \kappa}{\pi G \Sigma}, \tag{1}$$

where $c_s$ is the effective thermal speed of the disc, $\Sigma$ is the surface density and $\kappa$ is the epicyclic frequency (which, for a Keplerian disc, is equal to the angular velocity $\Omega$). The disc is unstable if $Q$ is smaller than a threshold value $\bar{Q} \approx 1$. It has been long recognized, especially in the context of galactic dynamics (Hohl 1971; Bertin & Romeo 1988), that the development of gravitational instabilities would lead to a self-regulation process: if the disc is initially cold, in the sense that $Q < \bar{Q}$, then gravitational instabilities would heat it up on the fast dynamical time-scale, bringing it toward stability; on the other hand, if the disc is hot enough to begin with, then radiative cooling is going to bring the value of $Q$ down toward an unstable configuration. As a result of the presence of these two competing mechanisms, the 'switch' associated with the onset of gravitational instabilities will act as a thermostat for the disc, which is therefore expected to be always close to marginal stability. A similar approach has been also suggested in the case of accretion discs (Paczyński 1978; Bertin 1997).

From the observational point of view, there are already some clues that the disc self-gravity can be important both in the context of protostellar discs and in accretion discs around supermassive black holes in active galactic nuclei (AGN). However, a detailed comparison with observations is limited by the lack of detailed models

★E-mail: giuseppe@ast.cam.ac.uk

of self-gravitating discs and by an incomplete understanding of the basic physical processes involved.

The importance of the disc self-gravity in observations of protostellar discs was pointed out by Adams, Lada & Shu (1988), who realized that a massive disc, with a flat rotation curve, could reproduce the observed flat long-wavelength spectral energy distribution (SED) of many protostellar sources. However, in these early studies no detailed model of self-gravitating accretion discs was available, so that the required disc mass turned out to be unreasonably large. These ideas were recently revisited by Lodato & Bertin (2001) in the light of a self-consistent disc model (Bertin & Lodato 1999), and they were able to model the observed SED of FU Orionis objects (a class of young stellar objects undergoing a phase of enhanced accretion), with a disc mass comparable to that of the central object. This model assumes that the outer disc (beyond a few au from the central star) is self-regulated. However, non-self-gravitating $\alpha$-models of accretion discs would predict a rapidly declining radial profile of $Q$, which would eventually become unphysically small in the outer regions of the disc. In the case of FU Orionis discs, the disc is predicted to be marginally stable already at a distance of $\approx$1 au from the central star (Bell & Lin 1994). The arguments at the basis of the self-regulation mechanisms would suggest that in the outer regions of the disc an additional heating source is required in order to keep the disc marginally stable. Lodato & Bertin (2001) argued that the difficulty with $\alpha$-models arises because these viscous models assume that energy dissipation is determined locally, whereas gravitational instabilities would naturally act in a global way, leading to a modification of the standard estimates of the viscous dissipation power.

Analogous considerations also hold in the context of AGN discs. Here, Lodato & Bertin (2003) have shown that the non-Keplerian rotation curve traced by water masers in the Seyfert galaxy NGC 1068 (Greenhill et al. 1996; Greenhill & Gwinn 1997) can be reproduced by self-regulated disc models. Sirko & Goodman (2003), following the same arguments of Lodato & Bertin (2001), have modelled the long-wavelength SED of AGN discs, based on the requirement that $Q \approx 1$. The latter authors also recognize the need for some additional heating, but, contrary to Lodato & Bertin (2001), attribute it to some 'external' source, namely nuclear fusion in stars embedded in the disc (see also Collin & Zahn 1999).

Actually, the issue of locality of transport in self-gravitating accretion discs still remains an open question. Lin & Pringle (1987) have suggested that the transport induced by self-gravity could be described within a viscous framework, and introduced a modified $\alpha$-prescription, where $\alpha \sim Q^{-2}$. In this way, a self-regulated disc would be characterized by a rather large effective viscosity, with $\alpha \approx 1$. On the other hand, Balbus & Papaloizou (1999) have shown that the energy equation for self-gravitating discs cannot be put in the form of a diffusion equation, as required in a viscous scenario, and that the energy flux contains some extra terms, associated with global wave transport, that are 'anomalous' from the point of view of viscosity. Similar ideas had also been suggested by Shu et al. (1990).

In this context, numerical simulations play a central role. Laughlin & Bodenheimer (1994) have performed global, smoothed particle hydrodynamics (SPH) simulations of massive isothermal discs, concluding that the density evolution of the disc could be reproduced in terms of simple $\alpha$-models. Laughlin & Różyczka (1996), using two-dimensional (2D) grid-based simulations, have shown that in order to reproduce the density evolution induced by gravitational instabilities an $\alpha$ coefficient dependent on radius was needed. However, these simulations did not include a detailed treatment of the heating and cooling processes in the disc, which have been shown to play a fundamental role in determining the outcome of the instability (Nelson et al. 2000; Pickett et al. 2000).

Gammie (2001) has performed local, shearing-sheet, zero-thickness simulations of self-gravitating discs, including a simple cooling term, and has concluded that a local description is adequate in such 'razor-thin' discs. However, Gammie's simulations are not appropriate to test global effects, because locality is set up from the beginning, and they are only valid for infinitesimally thin discs, while the typical distance over which gravitational instabilities are expected to travel scales with the disc thickness. Rice et al. (2003a,b) have already shown, using global, three-dimensional (3D) simulations, how global effects can be important in the dynamics of self-gravitating discs, in relation to the related issue of the fragmentation of a massive disc.

In this paper we present the results of global, 3D, SPH simulations of massive, cooling, non-magnetized discs. Our main purpose is to quantitatively determine the dissipation power provided by gravitational instabilities and to compare the results with the expectations based on a viscous theory of discs, in order to assess the extent to which the transport induced by gravitational instabilities can be regarded as a local process.

The paper is organized as follows. In Section 2 we summarize the basic transport properties of viscous and of self-gravitating discs, introducing the basic physical quantities involved. In Section 3 we describe the numerical set-up of our simulations. In Section 4 we show the results of our computations. In Section 5 we discuss our results in comparison with previous investigations and in relation to observed systems. In Section 6 we draw our conclusions. In Appendix A we discuss the more technical issue of transport induced by artificial viscosity in the numerical simulations presented.

## 2 TRANSPORT IN ACCRETION DISCS

In this section we will summarize a few well-known results about the dynamics of viscous and self-gravitating accretion discs, that are going to be essential in the description of our results. We will not go into the full details of the derivation of the main results, for which one can refer to standard reviews, such as that of Pringle (1981).

### 2.1 Non-self-gravitating discs

In the analysis performed in this paper we will adopt the thin disc approximation, and will therefore deal with vertically integrated quantities. The equations of motion for an axisymmetric disc, in cylindrical coordinates, are the equation of continuity

$$\frac{\partial \Sigma}{\partial t} + \frac{1}{R}\frac{\partial}{\partial R}(R\Sigma u) = 0, \tag{2}$$

and the azimuthal component of Euler's equation (expressed in terms of angular momentum conservation)

$$\frac{\partial}{\partial t}(\Sigma R^2 \Omega) + \frac{1}{R}\frac{\partial}{\partial R}(\Sigma R^3 \Omega u) = -\frac{1}{R}\frac{\partial}{\partial R}\left(R^2 T_{R\phi}\right), \tag{3}$$

where $u$ is the radial velocity and $T_{R\phi}$ is the relevant component of the viscous stress tensor, integrated in the vertical direction. This last term is the basic ingredient in the theory of accretion discs. As we have already anticipated, standard hydrodynamical viscosity is not sufficient to provide accretion at the required rates, and therefore $T_{R\phi}$ is generally described by means of ad hoc prescriptions. The $\alpha$-prescription (Shakura & Sunyaev 1973), based on simple

arguments on the relevant physical scales of turbulent cells in the discs, assumes that $T_{R\phi}$ is proportional to the disc pressure

$$T_{R\phi} = \left|\frac{\mathrm{d}\ln\Omega}{\mathrm{d}\ln R}\right|\alpha\Sigma c_\mathrm{s}^2, \tag{4}$$

where the proportionality constant $\alpha$ is an unknown parameter, usually considered to be smaller than unity. The $\alpha$-prescription can also be put in the following equivalent form, which involves the kinematical viscosity coefficient $\nu$

$$\nu = \alpha c_\mathrm{s} H, \tag{5}$$

where $H$ is the thickness of the disc.

The effect of viscosity on the energy balance is twofold: viscous torques convect energy between neighbouring annuli of the disc and they dissipate energy. The energy which is convected across a ring at radius $R$ per unit time is given by

$$\frac{\mathrm{d}E}{\mathrm{d}t} = 2\pi R^2 T_{R\phi}\Omega, \tag{6}$$

while the dissipation rate per unit surface is given by

$$D(R) = T_{R\phi}|R\Omega'|. \tag{7}$$

If the disc is in thermal equilibrium, we can derive a useful relation between the viscosity coefficient $\alpha$ and the cooling time-scale. If we assume that cooling can be simply parametrized in the following way

$$Q^- = \frac{U}{t_\mathrm{cool}} = \frac{\Sigma c_\mathrm{s}^2}{\gamma(\gamma-1)t_\mathrm{cool}}, \tag{8}$$

where $U$ is the internal energy per unit surface and $\gamma$ is the ratio of the specific heats, then, equating the viscous dissipation term, expressed in equation (7) to the cooling term, expressed in equation (8), leads to

$$\alpha = \left|\frac{\mathrm{d}\ln\Omega}{\mathrm{d}\ln R}\right|^{-2}\frac{1}{\gamma(\gamma-1)t_\mathrm{cool}\Omega}, \tag{9}$$

where we have also used equation (4).

### 2.2 Self-gravitating discs

We will now turn to the transport properties of self-gravitating discs. The gravitational potential due to the disc will be denoted by $\Phi_\mathrm{s}$, and $\boldsymbol{g} = -\nabla\Phi_\mathrm{s}$ is the gravitational field.

It can be shown (Lynden-Bell & Kalnajs 1972) that the equation of angular momentum conservation can be put in a form analogous to equation (3), as required in a viscous framework, where the gravitational stress tensor is

$$T_{R\phi}^\mathrm{grav} = \int \mathrm{d}z\frac{g_\mathrm{R}g_\phi}{4\pi G}. \tag{10}$$

Equation (10) only accounts for the transport induced by the gravitational field itself. Gravitational instabilities will also produce density and velocity perturbations that contribute to the transport and should be included in the calculations. This contribution (the 'Reynolds' stress) can be expressed as

$$T_{R\phi}^\mathrm{Reyn} = \Sigma\delta v_R\delta v_\phi, \tag{11}$$

where $\delta\boldsymbol{v} = \boldsymbol{v} - \boldsymbol{u}$ is the velocity fluctuation, with $\boldsymbol{v}$ the fluid velocity and $\boldsymbol{u}$ the mean fluid velocity.

Given an expression for the gravitational stress tensor, one could therefore be tempted to use the $\alpha$-prescription, and to assume that $T_{R\phi}$ is simply proportional to the local pressure. If large-scale structure and global processes play a role in self-regulating the disc, it could even be possible to give a 'generalized' $\alpha$-prescription, where $\alpha$ is to be determined by some global requirement (on this point, see Coppi 1980; Bertin 1997). In any case, even if such global parametrization is possible, it should be emphasized that the previous comments only apply to angular momentum transport. We still have to face the issue of energy transport in self-gravitating discs. In particular, we should check whether gravitational instabilities transport energy between neighbouring annuli according to equation (6) and whether they dissipate energy according to equation (7).

Balbus & Papaloizou (1999) have shown that, in general, energy transport cannot be described viscously. The energy balance equation for self-gravitating discs contains some 'extra' terms (see equation 59 in Balbus & Papaloizou 1999), that Balbus & Papaloizou ascribe to global wave transport. The important issue at this stage is to determine how important these extra terms are, and under which conditions they are able to influence the energy balance in the disc.

In this paper we use global numerical simulations in order to compute explicitly the different physical quantities described in this section. In particular, we will evaluate the gravitational stress tensor, according to equations (10) and (11), and the corresponding 'viscous' dissipation term, which can then be directly compared to the power actually dissipated in our simulated discs.

## 3 NUMERICAL SET-UP

### 3.1 The code

The 3D simulations presented here were performed using SPH, a Lagrangian hydrodynamic code (see Benz 1990; Monaghan 1992). In these simulations the central object is modelled as a point mass on to which gas particles can accrete if they approach to within the sink radius, while the gaseous disc is simulated using 250 000 SPH particles. Both the point mass and the gas particles use a tree to determine neighbours and to calculate gravitational forces (Benz 1990), and the central object is free to move under the influence of the disc gas. A significant saving in computational time is made by using individual, particle time-steps (Bate, Bonnell & Price 1995) with the time-steps for each particle limited by the Courant condition and by a force condition (Monaghan 1992).

Because the main aim of this work is to check the energy processes associated with gravitational instabilities, we explicitly solve the energy balance equation for the gas. We allow the disc to heat up due to both $P\mathrm{d}V$ work and viscous dissipation. The ratio of the specific heats is assumed to be $\gamma = 5/3$. For the cooling, we follow Gammie (2001) and add a simple cooling term to the energy equation. Specifically, we use the same type of parametrization as in equation (8). For a particle with internal energy per unit mass $u_i$, the cooling is implemented using

$$\frac{\mathrm{d}u_i}{\mathrm{d}t} = -\frac{u_i}{t_\mathrm{cool}}, \tag{12}$$

with $t_\mathrm{cool} = \beta\Omega^{-1}$. Gammie (2001) and Rice et al. (2003b) have shown that, for small cooling times, the disc may fragment into gravitationally bound objects while, for longer cooling times, the disc settles into a quasi-steady state with the imposed cooling balanced by dissipation through the growth of the gravitational instability. In particular, Gammie (2001) has shown that the fragmentation boundary occurs for $t_\mathrm{cool} \leqslant 3\Omega^{-1}$, while Rice et al. (2003b) show that global effects may lead to an enhanced tendency for fragmentation, so that the critical value for $t_\mathrm{cool}$ is increased. The reason why a disc that cools too rapidly is more prone to fragmentation is because gravitational heating of the disc occurs on the dynamical time-scale,

so if the disc cools very rapidly, self-gravity has not enough time to prevent the formation of bound objects in the disc. In our simulations we have adopted $\beta = 7.5$, in which case none of our discs should or was found to fragment.

### 3.2 Initial conditions

We consider a system comprising a central star, modelled as a point mass with mass $M_\star$, surrounded by a disc with mass $M_{\rm disc}$. We have performed three simulations with mass ratios $q = M_{\rm disc}/M_\star$, of 0.05, 0.1 and 0.25, respectively. The initial surface density profile is taken to be a power law $\Sigma \propto R^{-1}$, while the initial temperature profile is $T \propto R^{-1/2}$. The initial velocity profile is calculated by including the enclosed cylindrical mass when determining the angular frequency $\Omega$. With these initial conditions, the minimum value of $Q$ is attained at the outer edge of the disc. For each simulation the temperature normalization is chosen such that the minimum value of $Q$ is $Q_{\rm min} = 2$, and the whole disc is initially gravitationally stable. The disc is assumed to be in vertical hydrostatic equilibrium (see, for example, Pringle 1981), and we compute the scaleheight, $H$, using $H = c_{\rm s}/\Omega$ and distribute the particles such that the vertical density profile is a Gaussian. Actually, in a self-gravitating disc, the vertical density profile is not rigorously Gaussian (Bertin & Lodato 1999), so our initial set-up, strictly speaking, is not in dynamical equilibrium. However, dynamical equilibrium is achieved rapidly (i.e. in a dynamical time-scale) during the simulation.

Our calculations are essentially scale-free. In dimensionless units, the disc extends from $R_{\rm in} = 0.25$ to $R_{\rm out} = 25$, and we have taken $M_\star = 1$. In these units, one dynamical time-scale (orbital period) at $R = 1$ is equal to $2\pi$ code units. Therefore, one orbital period at the outer edge of the disc is roughly equal to 800 time units.

The disc is not initially in thermal equilibrium because the main source of heating, i.e. gravitational instabilities, is turned off because the disc is initially stable, while cooling is already effective. We follow our simulations for $\approx$5000 time units (i.e. approximately six orbital periods at the outer edge of the disc), by which stage the whole disc has reached thermal equilibrium.

### 3.3 Artificial viscosity: the Balsara switch

The standard SPH viscosity (e.g. Monaghan 1992) consists of a quadratic term similar to a Von Neumann–Richtmeyer viscosity (characterized by a dimensionless coefficient called $\beta_{\rm SPH}$) and a linear term that introduces a viscosity in shearing flows (characterized by a dimensionless coefficient called $\alpha_{\rm SPH}$). Because the goal of this work is to study transport associated with gravitational instabilities, we would like to reduce any angular momentum transport associated purely with the artificial viscosity (i.e. we wish to reduce the artificial shear viscosity).

Balsara (1995) suggested adding a shear correction term, known as the Balsara switch, to the standard SPH artificial viscosity which maintains the viscosity in compressional flows but reduces it to zero in pure shear flows. For all the simulations presented here we have used the Balsara form of the artificial viscosity and have used a value of 0.1 for the coefficient of the linear artificial viscosity term ($\alpha_{\rm SPH}$) and a value of 0.2 for the coefficient of the quadratic viscosity term. A detailed discussion of the transport of angular momentum induced by the chosen artificial viscosity is presented in Appendix A. Here we anticipate that the angular momentum transport induced by artificial viscosity is at least a factor of 10 smaller than that induced by gravitational instabilities in our simulated discs, and therefore plays a minor role in the dynamics of the disc.

## 4 RESULTS

### 4.1 General features

In all our simulations the disc initially cools down until the value of $Q$ becomes small enough for gravitational instabilities to become effective and to provide a source of effective heating. At later stages the disc settles into a quasi-steady state, where the heating provided by the instabilities balances the imposed cooling term. As predicted by the argument of self-regulation, this quasi-steady state is characterized by an almost constant value of $Q \approx 1$, over a wide radial range. The main features of the simulations are summarized in Figs 1–4.

Fig. 1 shows the surface density structure for the three simulations, with different total disc mass ($q = 0.05$, 0.1 and 0.25). The global structure induced by self-gravity is clearly seen in all three cases. The density enhancement in the spiral arms $\Delta\rho/\rho$ typically ranges between 2 and 4 in all cases. Already from this figure it can be noticed that, as the total disc mass increases, the pattern of the instability becomes progressively more dominated by low-$m$ modes. This is confirmed by the Fourier analysis shown in Fig. 2, that shows how, in the higher total mass cases, the modes with $m < 5$ dominate the structure. The Fourier amplitudes in Fig. 2 are computed as follows. We divide the disc in concentric rings of width $\Delta R = 2.5$ in dimensionless units. For each ring we then compute the mode amplitude $A_m$ as

$$A_m = \left| \sum_{i=1}^{N_{\rm ring}} \frac{{\rm e}^{-{\rm i}m\phi_i}}{N_{\rm ring}} \right|, \tag{13}$$

where $N_{\rm ring}$ is the number of particles in the ring, and $\phi_i$ is the azimuthal angle of the $i$th particle.

Fig. 3 shows the radial profile of $Q$ at three different times, towards the end of the simulation. The profile is not significantly altered with time, indicating that the simulations have reached thermal equilibrium, and are in a quasi-steady state. Actually, the fact that the self-regulated value of $Q$ turns out to be so close to unity in our simulations is quite remarkable. In fact, the marginal stability value $\bar{Q}$ is equal to unity only when the perturbation analysis is restricted to the case of the axisymmetric stability of an infinitesimally thin disc. The disc thickness has an important stabilizing effect, which leads to a lower temperature (and thus a lower value of $Q$) of the marginally stable state; on the other hand, even a light disc can be destabilized by the presence of swing amplified non-axisymmetric disturbances with high $m$ (for a discussion of these mechanisms see, for example, Bertin 2000). It then appears that these two competing effects basically counterbalance each other. A detailed investigation of the combined effect of these physical mechanisms in determining the precise value of $Q$ at marginal stability is, however, beyond the scope of the present paper.

Fig. 4 displays the initial and final radial profiles of the surface density (averaged in the azimuthal direction). It can be noticed that there is no significant evolution of the surface density at large radii. The major changes in the surface density occur close to the boundaries. In particular, there is a rapid drop in surface density close to the inner boundary. This is due to the fact that we have not attempted to give a detailed description of the boundary layer. The sudden lack of SPH particles at $R < 0.25$ causes an increased artificial pressure which pushes the inner particles into the sink radius of the star. This effect should be reduced with a more accurate description of the boundary layer. We have also checked that the total angular

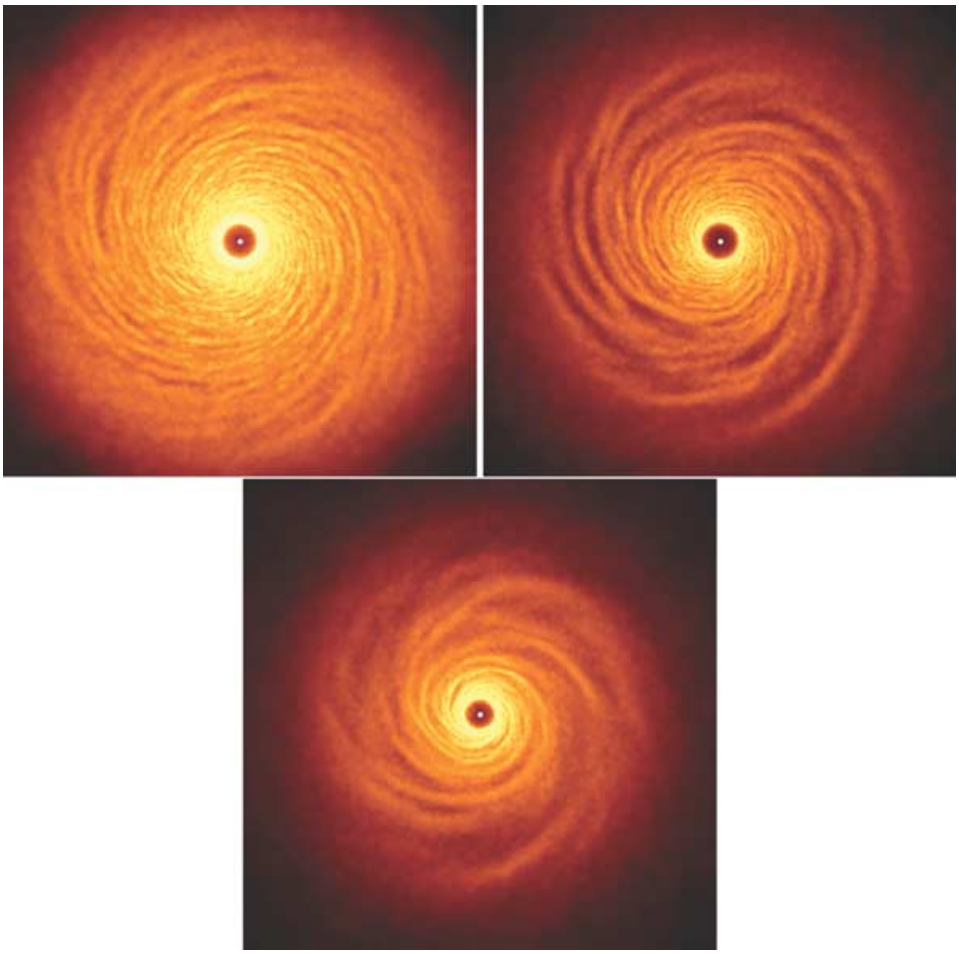

**Figure 1.** Surface density structure at the end of the simulations for (upper left) $q = 0.05$, (upper right) $q = 0.1$ and (bottom) $q = 0.25$.

momentum of the disc is conserved to within a few per cent throughout all the simulations.

When low values of the artificial viscosity are used, particle interpenetration might lead to a poor representation of strong shocks in SPH. This is not a serious issue in our case, because in our simulations only mildly supersonic shocks are involved. Based on the density contrast in the spiral arms, we estimate the Mach number of the shocks to be $\mathcal{M} \lesssim 1.5$. At these low values of $\mathcal{M}$, a value of $\beta_{\rm SPH} \approx 0.2$ is already sufficient to stop particle interpenetration (Bate 1995). This is confirmed by the well-defined spiral structure that we obtain (which would have been smeared out if significant particle interpenetration was indeed present), consistent with the results of previous simulations that used the standard SPH viscosity and higher values for the viscosity coefficients (Rice et al. 2003a,b).

### 4.2 Angular momentum transport and energy dissipation

The torque produced by gravitational instabilities in the disc is given by the sum of the two terms described in equations (10) and (11). After averaging the stress tensor azimuthally and radially, over a small region $\Delta R = 0.1$, we compute the corresponding value of $\alpha$ (see equation 4):

$$\alpha(R) = \left| \frac{{\rm d} \ln \Omega}{{\rm d} \ln R} \right|^{-1} \frac{\left\langle T^{\rm grav}_{R\phi} \right\rangle + \left\langle T^{\rm Reyn}_{R\phi} \right\rangle}{\Sigma c_{\rm s}^2}. \quad (14)$$

The resulting radial profiles of $\alpha$ are shown in Fig. 5 for the three cases $q = 0.05$, 0.1 and 0.25. The upper panels show separately the hydrodynamic and gravitational contributions to $\alpha$, while the bottom panels show the sum of the two. The plots show the time average of $\alpha$ at the end of the simulation, once the disc has reached a quasi-steady state. The time-averaging interval is 500 time units, i.e. 0.6 orbital times at the outer disc edge.

We can now use the general results of viscous disc theory outlined in Section 2 to test the locality of transport in our simulations. In fact, equation (9) gives us firm expectations for the value of $\alpha$ needed to balance the imposed cooling, if energy dissipation can be treated in a viscous framework, i.e. by using equation (7). In particular, in our simulations $t_{\rm cool}\Omega = \beta = 7.5$, $\gamma = 5/3$ and, because our discs are nearly Keplerian, ${\rm d} \ln \Omega / {\rm d} \ln R \approx -3/2$. Inserting these numbers in equation (9) would give us an expected value of $\alpha \approx 0.05$. It is important to note that the fact that the expected $\alpha$ turns out to be nearly independent on radius is a result of choosing the cooling time to be simply proportional to the dynamical time-scale. In the general case, of course, the resulting $\alpha$ need not be constant. The dotted line in Fig. 5 shows the expected value of $\alpha$. Our results are in fairly good agreement with the expectations of viscous transport theory.

It is also interesting to compare the dissipation rate $D(R)$ that would result if the transport process were viscous, i.e. computing $D(R)$ based on equation (7), with the actual dissipation rate. Because

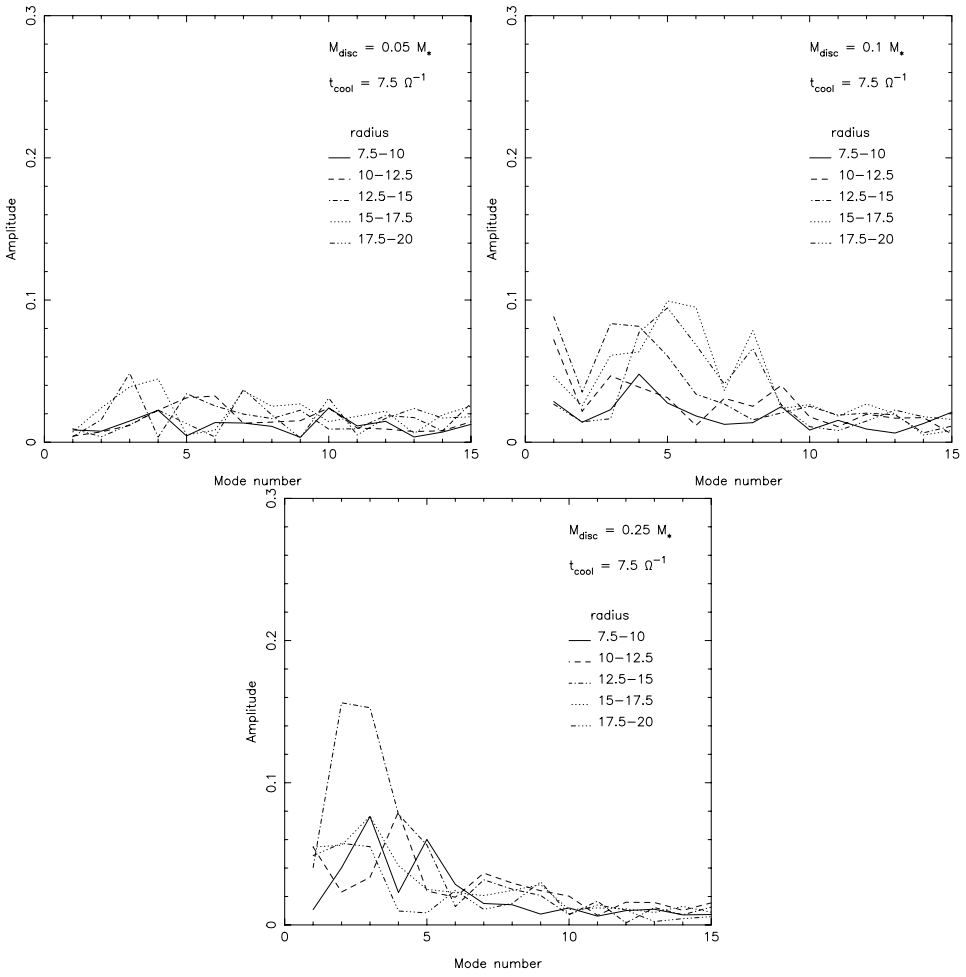


**Figure 2.** Amplitude of the first Fourier components of the density structure for different radial ranges in the three cases: (upper left) $q = 0.05$; (upper right) $q = 0.1$; (bottom) $q = 0.25$.

our discs are in thermal equilibrium, the dissipation rate can be obtained from the cooling rate using equation (8). This comparison is shown in Fig. 6, where the solid line shows $D(R)$ computed from equation (7), while the dotted line shows the cooling rate. Again, the plots show a good agreement with the expectations, the only exception being the outer parts of the most massive disc, where the actual dissipation rate seems to be slightly larger than that expected from a viscous process.

In general, our results indicate that, up to disc masses of $M_{\rm disc} = 0.25 M_\star$, gravitationally induced transport is reasonably well described within a local framework. This result could also be anticipated because the disc dynamics in all three simulations are dominated by rather high-$m$ modes, that dissipate on a short length-scale.

As a separate test for the locality of the transport, we have also computed $\alpha_{\rm part}(R, d)$, which we define as the gravitational part of $\alpha(R)$, taking into account only those particles inside a spherical radius $d$ from the radial point $R$ where we compute the stress. This quantity gives us a measure of the size of the region that has the most significant contribution to the gravitational stress at a given point. However, it should be kept in mind that this quantity only accounts for the stress produced by the gravitational field, without including the hydrodynamical component.

Fig. 7 shows the results for $R = 15$ for the three simulations. The upper panel shows clearly that the more massive the disc, the more distant regions from the point contribute to the stress. However, it should be noted that, because in the thermal equilibrium state $Q \approx 1$ in all three cases, a more massive disc is also characterized by a larger value of the effective thermal speed $c_{\rm s}$, and is therefore thicker. Because we expect that gravitational disturbances propagate over a length-scale of the order of the thickness of the disc, to compare appropriately the results of the three simulations, we should check the dependence of $\alpha_{\rm part}$ on $d/H$. This is shown in the bottom panel of Fig. 7. In all cases, more than 80 per cent of the contribution to the gravitational torque comes from a region with size $\Delta \approx 10H$. Transport is local if $\Delta \ll R$. We can therefore conclude that angular momentum transport is determined by local conditions only for discs with $H/R \ll 0.1$. When $Q \approx 1$, the ratio $H/R$ is proportional to $M_{\rm disc}/M_\star$, which means that sufficiently massive discs may violate the previous condition. Actually, our most massive disc (for which $M_{\rm disc}/M_\star = 0.25$) only marginally satisfies $H/R < 0.1$. Indeed, as can be seen from Figs 5 and 6, global wave transport might play some role in the outer disc, in this case.

## 5 DISCUSSION

### 5.1 Comparison with previous work

The distinctive feature of the present work is that we have performed global, 3D simulations of massive discs, including the detailed

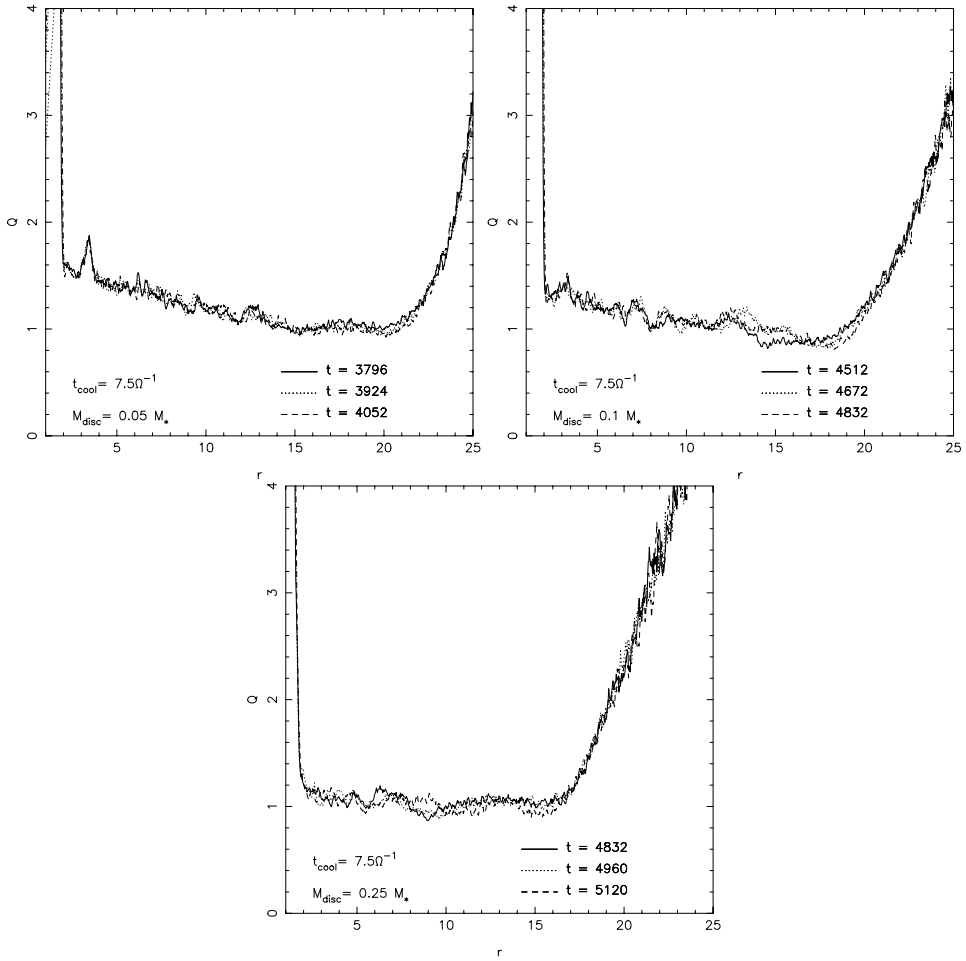


**Figure 3.** Profiles of the $Q$ parameter for the three simulations: (upper left) $q = 0.05$; (upper right) $q = 0.1$; (bottom) $q = 0.25$.

effects of heating from gravitational instabilities and cooling. Our simulations are similar to those performed by Rice et al. (2003a,b), with the difference that these previous investigations were concerned about either the motion of the central object caused by the massive disc, or the issue of fragmentation of the disc, while here the main goal is to characterize the transport properties induced by gravitational instabilities.

We believe that both performing 3D simulations and solving explicitly the energy equation are essential to determine the final outcome of the instabilities. In fact, the dynamical properties of self-gravitating discs are determined to a large extent by the process of self-regulation, which is strongly dependent on the detailed heating and cooling mechanisms, as outlined in the introduction. Furthermore, because one of the main tests we want to perform is to check the type of dissipative process associated with gravitational instabilities, solving the energy equation is essential. The requirement of 3D simulation is also fundamental, because the typical size of gravitational disturbances is related to the disc thickness, so that any zero-thickness simulation will automatically lead to an underestimate of global effects.

Previous numerical work carried out on the subject includes: global, 3D SPH simulations of massive isothermal discs (Laughlin & Bodenheimer 1994); global, 2D SPH simulations with detailed heating and cooling (Nelson et al. 2000); global, 3D grid-based simulations with heating and cooling (Pickett et al. 2000); and local, 2D grid-based simulations with heating and cooling (Gammie 2001). In this section we describe the similarities and the differences between our study and these previous studies.

One of the first studies of gravitational instabilities in discs was performed by Laughlin & Bodenheimer (1994). They modelled a very massive disc (with $M_{\rm disc} \approx M_\star$) and followed its evolution with a 3D SPH code, without including any heating or cooling term, but simply assuming that the disc was locally isothermal. In this study, the authors also tried to give a detailed characterization of the transport. Their approach was however slightly different to ours, in that they evolved their simulation long enough to capture the viscous evolution of the disc, and then compared the evolution of the azimuthally averaged surface density with simple one-dimensional viscous models, concluding that the disc evolution could be well reproduced by a viscous model with $\alpha \approx 0.03$. This work is important because it clarifies that gravitational instabilities are actually able to transport angular momentum efficiently and that the surface density evolution is indeed of a diffusive nature, as expected (see Section 2), but does not answer the important question of whether energy dissipation is local or global.

Nelson et al. (2000) performed 2D simulations with particular emphasis on the cooling processes in the disc and included a more realistic cooling function than the simple parametrization adopted here. Their disc mass was $M_{\rm disc} = 0.2 M_\star$, very similar to our most massive case. They estimated the effective $\alpha$ associated with

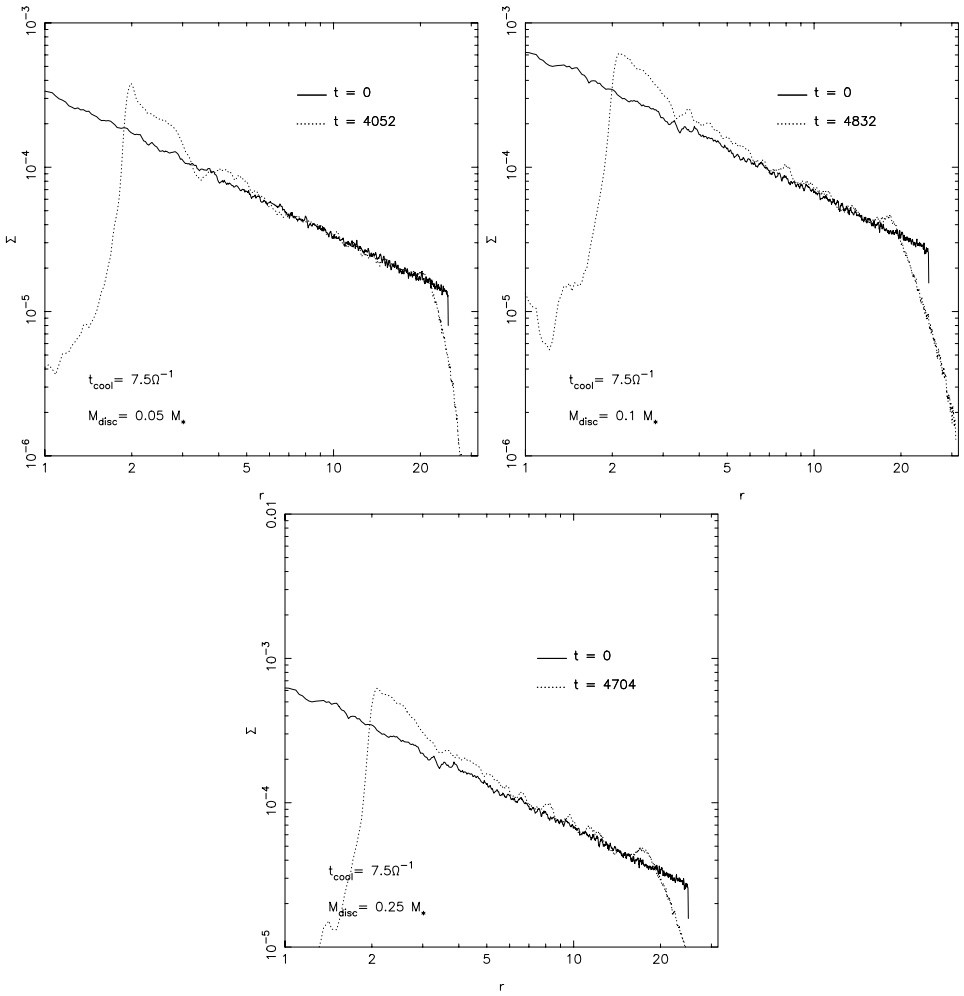


**Figure 4.** Radial profiles of the surface density at the end of the three simulations: (upper left) $q = 0.05$; (upper right) $q = 0.1$; (bottom) $q = 0.25$. The solid line shows the initial surface density profile.

artificial viscosity (see Section 3.3) to be of the order of $5 \times 10^{-3}$, comparable to the expectations based on equations (A1) and (A2), and an order of magnitude smaller than what we obtain here from transport induced by gravitational torques. Indeed, in our simulations most of the angular momentum is carried by collective instabilities and by gravitational torques, rather than by the artificial shear. Comparing the dissipation rates from shock heating with that from turbulent heating in their simulations, Nelson et al. (2000) conclude that, at least in the outer disc, gravitational torques should not contribute more than the torques associated with artificial viscosity, while in our simulation gravitational torques are everywhere dominant. A possible reason for this discrepancy lies in the 3D nature of our simulations, which may allow gravitational disturbances to travel further and allows low-$m$ modes to be more prominent. Actually, even if the mode amplitudes that we obtain here (see Fig. 2) are in rough agreement with those obtained by Nelson et al. (2000), they find very similar mode amplitudes for all modes with $m < 8$, while in our case there is a marked increase of mode amplitude for modes with $m < 5$ (see Fig. 2).

Gammie (2001) performed an analysis very similar to our own (actually, we adopt the same prescription for the cooling term, see equation 12). The main difference is that Gammie's simulations are local and 2D, while ours are global and 3D. He computes the effective $\alpha$ based on equation (14), as we do. The main results that we obtain are basically in agreement with Gammie's results, in that the expected value of $\alpha$ from a viscous theory of discs is very close to the computed value in the simulations. However, by using a global approach, we are now able to check how these results depend on the total disc mass and on the disc thickness, whereas Gammie could only extrapolate his results to thicker configurations.

Recently, Johnson & Gammie (2003) have extended the work of Gammie (2001) to include a more realistic cooling function in 2D simulations. Actually, the use of detailed cooling functions makes it even more important to perform a full 3D simulation, because most of the radiative transport will occur in the vertical direction, so that using vertically averaged values for the relevant physical quantities, as done by Johnson & Gammie (2003), might lead to incorrect results.

### 5.2 Impact on observed systems

It is now commonly accepted that most low-mass young stellar objects possess a circumstellar disc, with lifetimes of at least 1 Myr. Circumstellar discs play an important role in the process of star formation and are believed to be the site where planet formation occurs. Observational evidence for the presence of such discs is either

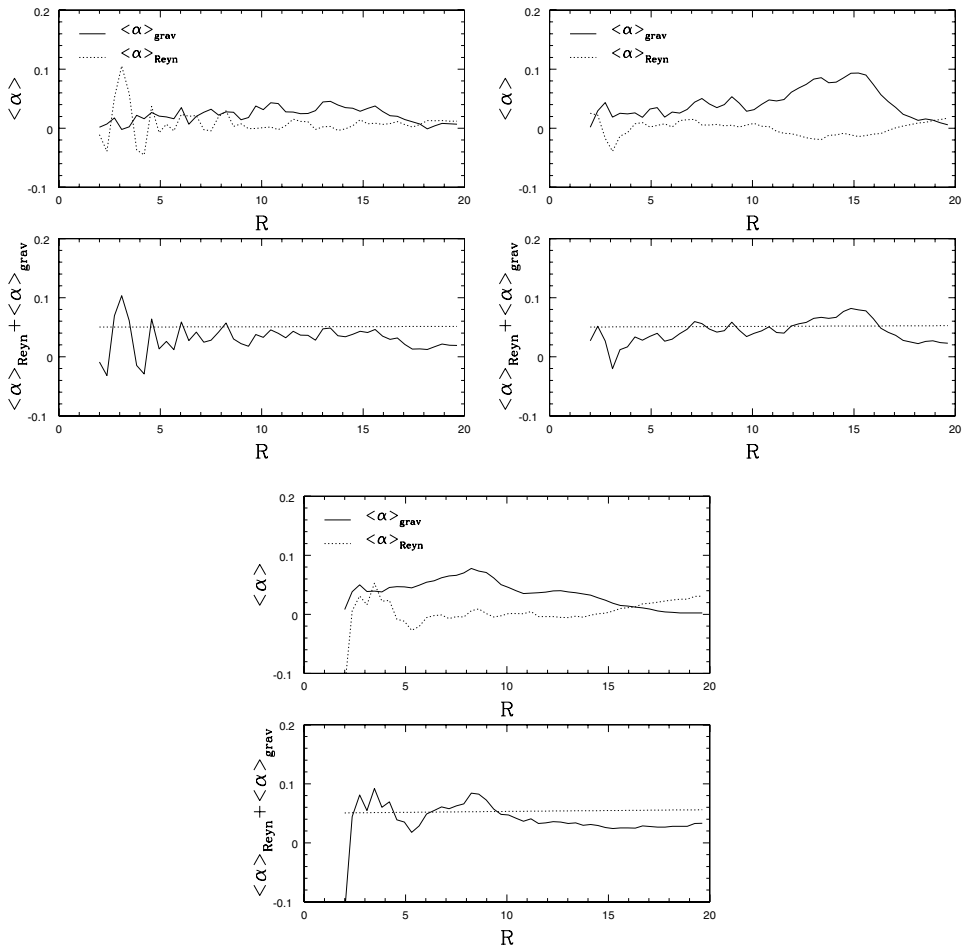


**Figure 5.** Effective $\alpha$ produced by gravitational instabilities for (upper left) $q = 0.05$, (upper right) $q = 0.1$ and (bottom) $q = 0.25$. The top panel shows the separate contribution of $\alpha_{\rm grav}$ and $\alpha_{\rm Reyn}$, and the lower panel shows the sum of the two contributions compared with the expected value from a local viscous model (dotted line).

indirect, i.e. based on the disc emission at long wavelengths, such as in the infrared (starting from Adams et al. 1988) and at submillimetre (submm) wavelengths (Beckwith et al. 1990), or direct, i.e. by imaging of silhouette discs in the Orion nebula (McCaughrean & O'Dell 1996). Especially in the earliest phases of star formation these discs might be fairly massive; for example, Launhardt & Sargent (2001), using submm observations, report the discovery of a massive disc (with $M_{\rm disc}/M_\star \gtrsim 0.3$) in a very young (class I) protostellar object. There are also some indications that the discs in FU Orionis objects might be fairly massive; Sandell & Weintraub (2001) report $M_{\rm disc}/M_\star \gtrsim 0.1$ in most of the FU Orionis discs they have observed. As already mentioned, detailed modelling of FU Orionis outbursts produces radial profiles of $Q$ that fall below unity already at a distance of $\approx$1 au from the central object (Bell & Lin 1994). All these systems are likely to be affected by self-gravity that, if indeed energy dissipation is non-local, may produce some observable modification in the SED. It is then interesting to see that the models by Bell & Lin (1994) predict $H/R \gtrsim 0.1$, which, according to the results of this work, are large enough for non-local effects to become important, as suggested by Lodato & Bertin (2001).

In the context of AGN discs, the distance at which the disc becomes marginally stable to gravitational instabilities is typically of the order of $10^3 R_{\rm g}$ (Lodato & Bertin 2003), where $R_{\rm g}$ is the gravitational radius of the black hole. Water maser emission (Greenhill & Gwinn 1997) and radio continuum observations (Gallimore et al. 1997) show that in many cases the disc can extend to radii much larger than that, thus allowing self-gravity to influence the disc structure. In this context, self-regulated models have been applied both to the modelling of the SED (Sirko & Goodman 2003) and to the modelling of the rotation curve in the outer disc of the Seyfert galaxy NGC 1068 (Lodato & Bertin 2003). Johnson & Gammie (2003) use their 2D results with 'realistic' cooling (see Section 5.1) to argue that the disc model proposed by Lodato & Bertin (2003) for NGC 1068 would be subject to fragmentation, but unfortunately Johnson & Gammie (2003) do not explore the region of the parameter space relevant to the Lodato & Bertin model.

As a final comment, we note that the present work refers to the situation where the dominant source of transport and dissipation is provided by gravitational instabilities. In observed systems, other sources of transport could be present, which might reduce the effect of gravitational instabilities.

## 6 CONCLUSIONS

In this paper we have investigated the transport properties induced by disc self-gravity in relatively massive accretion discs. In particular, we have discussed the extent to which angular momentum transport

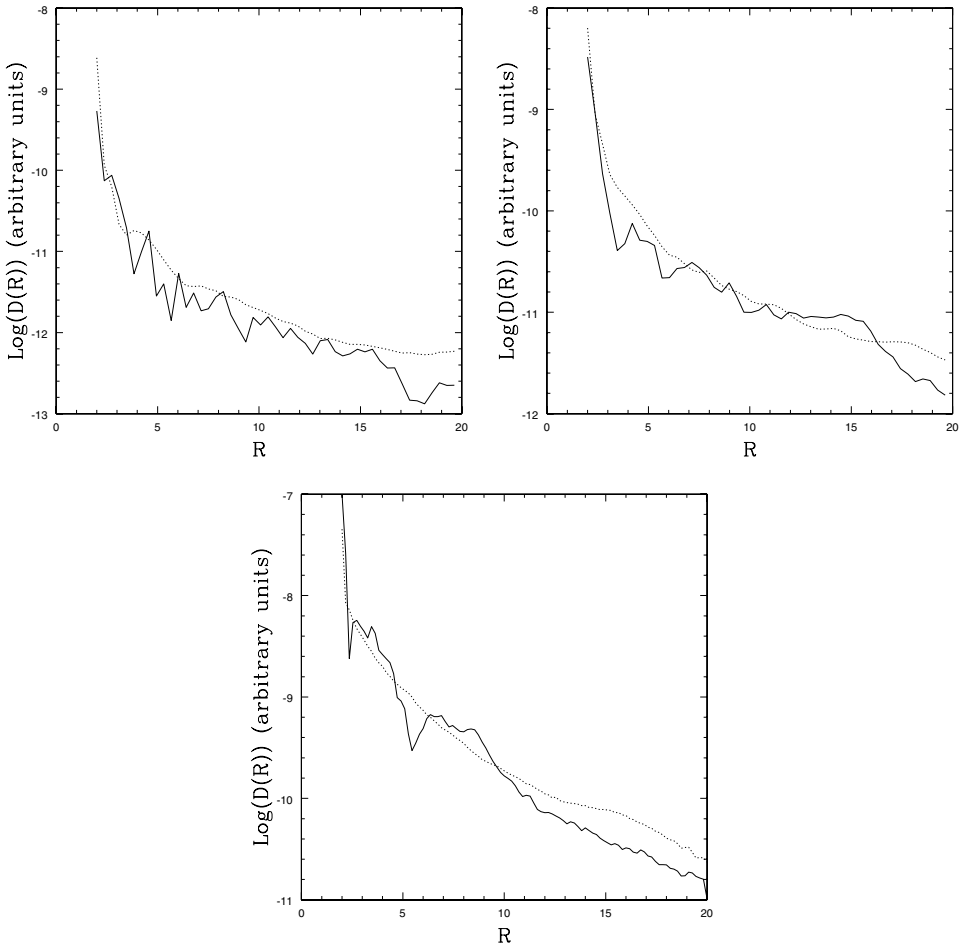


**Figure 6.** Viscous dissipation rate (solid line, from equation 7) and actual cooling rate (dotted line) for (upper left) $q = 0.05$, (upper right) $q = 0.1$ and (bottom) $q = 0.25$.

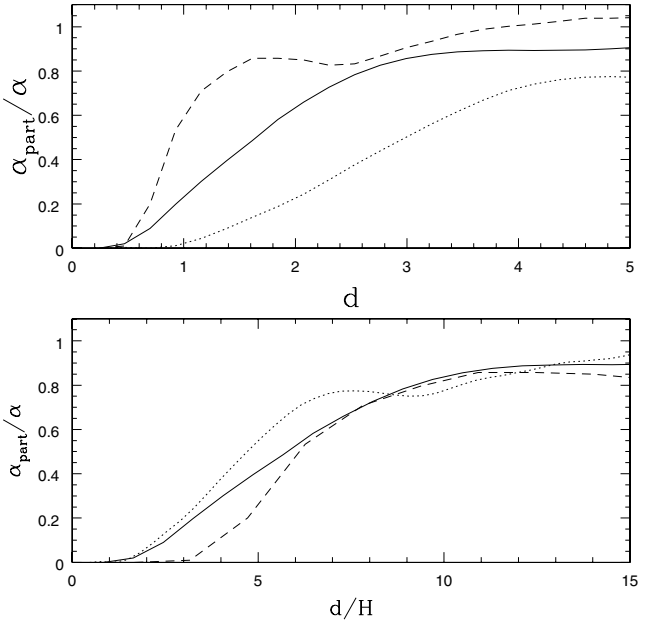


**Figure 7.** Contribution to the stress at $R = 15$ from regions of the discs at a distance $<d$ from $R$: dashed line, $q = 0.05$; solid line, $q = 0.1$; dotted line, $q = 0.25$.

and energy dissipation can be described within a viscous framework. To this goal, we have performed global, 3D simulations using SPH.

Most of the recent work on the subject has focused on the issue of the conditions for disc fragmentation, especially in relation to the process of planet formation in protostellar discs (Boss 2002; Mayer et al. 2002; Rice et al. 2003b), or massive star formation in AGN discs (Levin 2003; Goodman & Tan 2004). Here, we would like to check the behaviour of self-gravitating discs in the case where fragmentation does not occur and the disc evolves towards a quasi-steady state where cooling is balanced by heating from gravitational instabilities.

The issue of the transport properties induced by gravitational instabilities has been discussed analytically in the past by Lynden-Bell & Kalnajs (1972) and, more recently, by Balbus & Papaloizou (1999). There are two major aspects of the problem, as follows. (i) To what extent is the shear stress $T_{R\phi}$ at a given radius $R$ determined by local conditions? This point directly calls into question the use of the $\alpha$ formalism, which explicitly requires that $T_{R\phi}$ is only dependent on the local values of density and thermal velocity (see also the discussion in Section 2.2). (ii) The second aspect is whether energy transport is only determined by the gravitationally induced shear stress or whether instead global wave transport occurs, hence influencing energy dissipation in the disc, as argued by Balbus & Papaloizou (1999).

We have performed several simulations, with different values of the ratio $M_{\rm disc}/M_\star$, to test how the global transport properties of the disc change with increasing total disc mass. Our simulations appear to evolve to a quasi-steady state, characterized by an almost flat profile of the axisymmetric stability parameter $Q \approx 1$, in which the heating provided by gravitational instabilities balances the imposed cooling rate. We have computed the torque induced by gravitational instabilities and the corresponding viscous dissipation rate, which we then compare to the actual dissipation rate in our simulated discs. We have found values of $\alpha \approx 0.05$, in reasonable agreement with the expectation from a viscous theory. Energy dissipation in our simulations is also fairly well described using a viscous approach. These results directly address aspect (ii), described above, and confirm the argument of Balbus & Papaloizou (1999), who had indeed argued that for 'self-regulated' discs, in which $Q \approx 1$, global wave transport of energy would not play a major role.

On the other hand, we have indeed noticed that more massive discs tend to be dominated by lower $m$ modes, leading to a more global pattern of the gravitational disturbances. We have also been able to determine the size of the region that mostly contributes to the torque at a given point in the disc. More than 80 per cent of the torque is produced within a region of size $\Delta \approx 10H$, where $H$ is the thickness of the disc. These results directly address issue (i), described above. We can therefore conclude that a viscous description of the transport in self-gravitating discs is only appropriate when $H/R \lesssim 0.1$. In systems like FU Orionis, where models predict disc thickness $\approx$0.1 (Bell & Lin 1994), global effects could play a role and modify the dissipation rates in the outer disc.

The results of this work should be extended both toward a more thorough investigation of the parameter space (in particular, it is very important to test the transport properties of discs more massive than $0.25M_\star$, and to explore the results obtained with different initial conditions and cooling time-scale, which in the present work has been taken to be $t_{\rm cool} = 7.5\Omega^{-1}$), and toward a more realistic description of the cooling function; see, for example, Nelson et al. (2000) and Johnson & Gammie (2003).

## ACKNOWLEDGMENTS

The simulations presented in this work were performed using the UK Astrophysical Fluid Facility (UKAFF). We thank C. Clarke, J. Pringle and G. Bertin for several interesting discussions and for a careful reading of the manuscript. WKMR acknowledges support from a UKAFF Fellowship.

## REFERENCES

Adams F. C., Lada C. J., Shu F. H., 1988, ApJ, 326, 865
Armitage P. J., Livio M., Pringle J. E., 2001, MNRAS, 324, 705
Artymowicz P., Lubow S. H., 1994, ApJ, 421, 651
Balbus S. A., Hawley J. F., 1998, Rev. Mod. Phys., 70, 1
Balbus S. A., Papaloizou J. C. B., 1999, ApJ, 521, 650
Balsara D. S., 1995, J. Comput. Phys., 121, 357
Bate M., 1995, PhD thesis, Univ. Cambridge
Bate M. R., Bonnell I. A., Price N. M., 1995, MNRAS, 277, 362
Beckwith S. V. W., Sargent A. I., Chini R. S., Guesten R., 1990, AJ, 99, 924
Bell K. R., Lin D. N. C., 1994, ApJ, 427, 987
Benz W., 1990, in Buchler J., ed., The Numerical Modelling of Nonlinear Stellar Pulsations. Kluwer, Dordrecht, p. 269
Bertin G., 1997, ApJ, 478, L71
Bertin G., 2000, Dynamics of Galaxies. Cambridge Univ. Press, Cambridge
Bertin G., Lodato G., 1999, A&A, 350, 694
Bertin G., Romeo A. B., 1988, A&A, 195, 105
Boss A. P., 2002, ApJ, 576, 462
Collin S., Zahn J. P., 1999, A&A, 344, 433
Coppi B., 1980, Comments on Plasma Physics and Controlled Fusion, 5, 261
Gallimore J. F., Baum S. A., O'Dea C. P., 1997, Nat, 388, 852
Gammie C. F., 1996, ApJ, 457, 355
Gammie C. F., 2001, ApJ, 553, 174
Goodman J., Tan J. C., 2004, ApJ, in press (astro-ph/0307361)
Greenhill L. J., Gwinn C. R., 1997, Ap&SS, 248, 261
Greenhill L. J., Gwinn C. R., Antonucci R., Barvainis R., 1996, ApJ, 472, 21
Hohl F., 1971, ApJ, 168, 343
Johnson B. M., Gammie C. F., 2003, ApJ, 597, 131
Laughlin G., Bodenheimer P., 1994, ApJ, 436, 335
Laughlin G., Ròżyczka M., 1996, ApJ, 456, 279
Launhardt R., Sargent A. I., 2001, ApJ, 562, 173
Levin Y., 2003, preprint (astro-ph/0307084)
Lin D. N. C., Pringle J. E., 1987, MNRAS, 225, 607
Lodato G., Bertin G., 2001, A&A, 375, 455
Lodato G., Bertin G., 2003, A&A, 398, 517
Lynden-Bell D., Kalnajs A. J., 1972, MNRAS, 157, 1
Lynden-Bell D., Pringle J. E., 1974, MNRAS, 168, 603
McCaughrean M. J., O'Dell C. R., 1996, AJ, 111, 1977
Mayer L., Quinn T., Wadsley J., Stadel J., 2002, Sci, 298, 1756
Monaghan J. J., 1992, ARA&A, 30, 543
Murray J. R., 1996, MNRAS, 279, 402
Navarro J., Steinmetz N., 1997, ApJ, 478, 13
Nelson A. F., Benz W., Ruzmaikina T. V., 2000, ApJ, 529, 357
Paczyński B., 1978, Acta Astron., 28, 91
Pickett B. K., Cassen P., Durisen R. H., Link R., 2000, ApJ, 529, 1034
Pringle J. E., 1981, ARA&A, 19, 137
Rice W. K. M., Armitage P. J., Bate M. R., Bonnell I. A., 2003a, MNRAS, 338, 227
Rice W. K. M., Armitage P. J., Bate M. R., Bonnell I. A., 2003b, MNRAS, 339, 1025
Sandell G., Weintraub D., 2001, ApJ, 134, 115
Shakura N. I., Sunyaev R. A., 1973, A&A, 24, 337
Shu F., Tremaine S., Adams F. C., Ruden S. P., 1990, ApJ, 358, 495
Sirko E., Goodman J., 2003, MNRAS, 341, 501
Thacker R. J., Tittley E. R., Pearce F. R., Couchman H. M. P., Thomas P. A., 2000, MNRAS, 319, 619
Toomre A., 1964, ApJ, 139, 1217

## APPENDIX A: ANGULAR MOMENTUM TRANSPORT INDUCED BY ARTIFICIAL VISCOSITY

In this appendix we discuss the magnitude of the angular momentum transport associated with the artificial SPH viscosity, in order to be sure that the main contribution to the shear stress described in Section 4 is actually due to the effect of gravitational disturbances.

### The Balsara switch

As mentioned in the main text, we have adopted the Balsara form of viscosity in order to reduce the effect of artificial viscosity in transporting angular momentum. Although this modification to the standard SPH viscosity has been studied in some detail (Navarro & Steinmetz 1997; Thacker et al. 2000), it would be useful to have some idea of the reduction in shear viscosity that occurs when using this form of the artificial viscosity.

In the continuum limit, the linear term in the standard SPH artificial viscosity can be shown to have the following form (Artymowicz & Lubow 1994; Murray 1996)

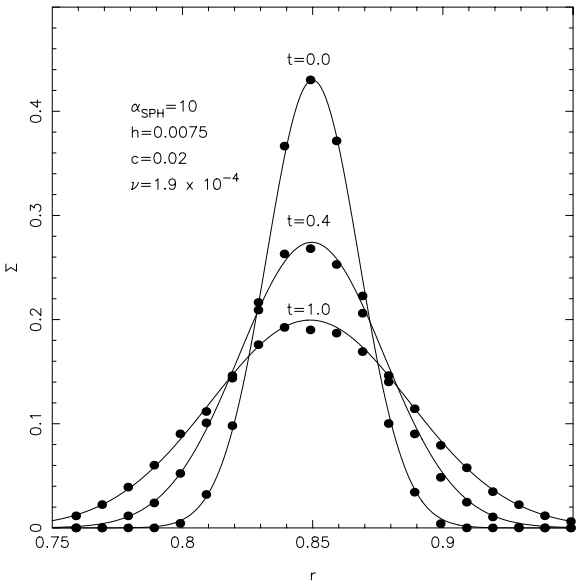


**Figure A1.** Radial surface density plots at times of $t = 0.0$, $t = 0.4$ and $t = 1.0$ for an axisymmetric ring evolved using SPH with the standard artificial viscosity (dots) and evolved analytically (solid lines) with a viscosity determined using the parameters of the SPH calculation.

$$\nu = \frac{1}{8}\alpha_{\rm SPH} c_{\rm s} h, \tag{A1}$$

where $\alpha_{\rm SPH}$ is the linear viscosity coefficient, $c_{\rm s}$ is the sound speed and $h$ is the SPH smoothing length (which essentially determines the resolution of the simulation). As shown by Lynden-Bell & Pringle (1974), the time evolution of the surface density and radial velocity of an initial Gaussian ring can be determined analytically. To test the standard SPH viscosity, Murray (1996) therefore considered the evolution of an initial Gaussian ring with the initial radial velocity determined analytically, using equation (A1) to determine the viscosity. We have repeated this calculation and show the results in Fig. A1. The SPH calculation had a linear viscosity coefficient of $\alpha_{\rm SPH} = 10$, a sound speed of $c_{\rm s} = 0.02$, and a constant smoothing length of $h = 0.0075$. The choice of the SPH parameter was made in order to be consistent with Murray (1996). As in Murray (1996), the pressure forces were switched off so as to study the artificial viscosity in isolation. This, on the one hand, prevents the ring from spreading due to pressure forces, but on the other hand would cause the disc to collapse to the mid-plane. As a check that converging flows do not influence our results, we have also performed some tests with a fixed vertical coordinate of the SPH particles, and we found no significant differences. The dots in Fig. A1 show the time evolution of the SPH surface density. For the chosen SPH parameters, the associated shear viscosity, according to equation (A1), is $\nu = 1.9 \times 10^{-4}$. The solid lines in Fig. A1 show the analytical viscous evolution of an initial Gaussian ring with an imposed shear viscosity of $\nu = 1.9 \times 10^{-4}$. As in Murray (1996) the SPH evolution of the initial Gaussian ring follows the analytical result very closely and equation (A1) appears to be a good representation of the shear viscosity associated with the linear term in the standard SPH artificial viscosity.

To perform a similar calculation to determine the viscous transport when using the Balsara switch is more subtle because the shear viscosity should, ideally, go to zero. This will, of course, not be exactly true in practice, but we cannot now determine what the initial radial velocity profile should be. To get some idea of the viscous transport when using the Balsara switch, we have considered the time evolution of a Gaussian ring in which, because ideally we expect no shear viscosity, we set the initial radial velocities to zero. For linear viscosity coefficients of $\alpha_{\rm SPH} = 0.1$ and $\alpha_{\rm SPH} = 1$ there is no noticeable spreading between $t = 0$ and $t = 1$. For $\alpha_{\rm SPH} = 10$, however, the ring did spread slightly. The left-hand side of Fig. A2 shows the SPH evolution of an initial Gaussian ring (dots) plotted at times of, as in Fig. A1, $t = 0.0$, 0.4 and 1 for $\alpha_{\rm SPH} = 10$. A direct comparison with the analytical prediction for the surface density evolution and with the results shown in Fig. A1 would be misleading in this case, because initially the ring has to settle down before attaining the appropriate radial velocities resulting from the viscous evolution. As a result, the initial evolution of the ring is slower than predicted analytically by Lynden-Bell & Pringle (1974). In the left panel of Fig. A2 we also plot the analytical evolution of an initial Gaussian ring (solid line) with an imposed viscosity of $\nu = 8.0 \times 10^{-6}$, which appears to best describe the average evolution of the ring. In order to compare these results with those obtained from the use of the standard SPH viscosity, we performed an identical calculation (with the initial radial velocities set to zero) except using the standard SPH viscosity without the Balsara switch. This is shown in the right-hand side of Fig. A2. Again the dots represent the evolution of the SPH surface density at times of $t = 0.0$, 0.4 and 1, and the solid line shows the analytical evolution of the surface density. Also in this case, as discussed above, the initial evolution is slower than expected. The average evolution between

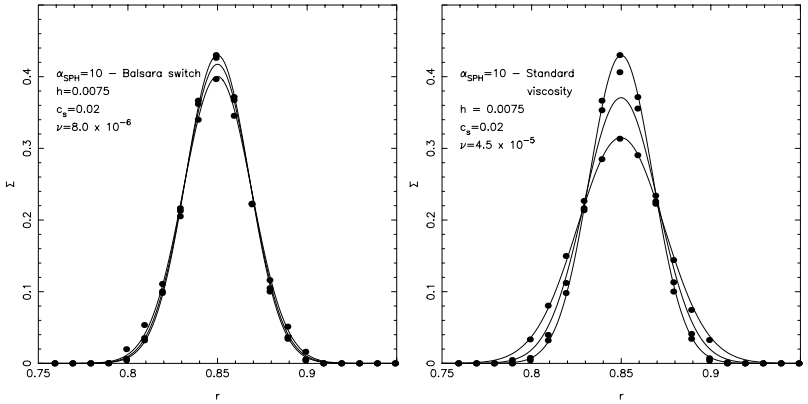


**Figure A2.** Radial surface density plots at times of $t = 0.0$, $t = 0.4$ and $t = 1.0$ for an axisymmetric ring evolved using SPH (dots) and evolved analytically (solid lines). In the left-hand figure the Balsara switch was used in the SPH artificial viscosity while in the right-hand figure the simulation was evolved using the standard SPH viscosity. The Balsara switch clearly reduces the effective shear viscosity by a factor of between 5 and 10.

$t = 0$ and $t = 1$ can be fitted with a viscosity $\nu = 4.5 \times 10^{-5}$. These results, although not conclusive, indicate that the Balsara switch reduces the effective shear viscosity by a factor of between 5 and 10. By using the Balsara switch we should therefore be able to reduce the angular momentum transport due to the artificial shear viscosity without, according to Thacker et al. (2000), significantly influencing the handling of shocks.

A comparison between equations (A1) and (5) readily shows that the artificial shear viscosity in SPH (not using the Balsara switch) can be described in terms of the $\alpha$ parametrization in the following way:

$$\alpha_{\rm art} = \frac{1}{8}\alpha_{\rm SPH}\frac{h}{H}. \tag{A2}$$

Equation (A2) therefore shows that the magnitude of $\alpha_{\rm art}$ depends on how well the vertical structure of the disc is resolved. In most of our simulations we typically had $H \approx 5h$, so that, if we had used the normal SPH viscosity, we would expect $\alpha_{\rm art} \approx 2.5 \times 10^{-3}$, for $\alpha_{\rm SPH} = 0.1$ (the value used in all our simulations). The use of the Balsara switch enables us to further reduce this contribution to $\alpha_{\rm art} \approx 5 \times 10^{-4}$.

### Artificial transport in disc simulations

As discussed in Appendix A1, thanks to the Balsara switch, we expect the linear term in the viscosity to produce only a minor contribution to the shear stress. However, the quadratic term of the artificial viscosity (parametrized by $\beta_{\rm SPH}$) might still give some contribution to the angular momentum transport. In addition, in our self-gravitating disc simulations, we have also added pressure force, which might as well contribute to the stress, as found also by Murray (1996). Moreover, we would also like to test this issue in a less idealized case, with respect to the simple spreading ring calculations described in Appendix A1. For this purpose, we have performed some simulations, taking the same surface density profile as in Section 4 (i.e. $\Sigma \propto R^{-1}$) and a constant $Q$ profile, with $Q = 1$, but in which we have switched off the main source of transport and dissipation (i.e. the disc self-gravity) and the cooling. The artificial viscosity coefficients were $\alpha_{\rm SPH} = 0.1$ and $\beta_{\rm SPH} = 0.2$, as in the simulations presented in Section 4. We have computed the Reynolds stress according to equation (11), and obtained an effective $\alpha_{\rm art}$ from equation (4). The results are shown in Fig. A3. The magnitude of this artificial transport is never larger than $\alpha_{\rm art} \approx 5 \times 10^{-3}$. Because our results (see Section 4) indicate that the transport induced by gravitational torques can be parametrized with an effective $\alpha \approx 5 \times 10^{-2}$, we can be confident that the major contribution to the stress tensor comes from gravitational torques rather than from artificial viscosity.

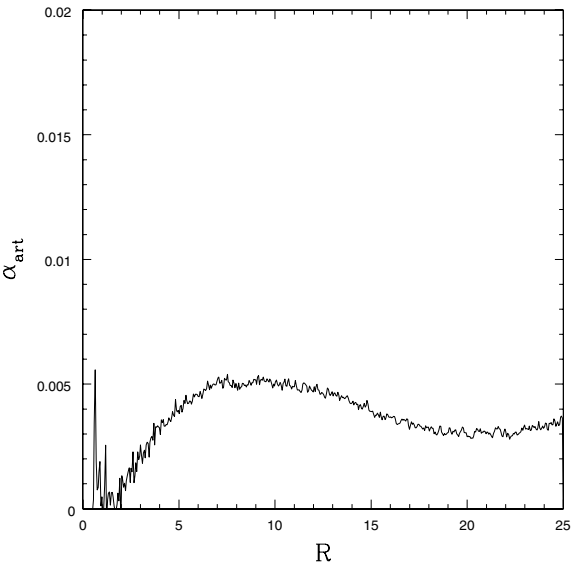


**Figure A3.** Angular momentum transport induced by artificial viscosity in our SPH simulations, as parametrized by an effective $\alpha_{\rm art}$.

This paper has been typeset from a TEX/LATEX file prepared by the author.